Nat. Hazards Earth Syst. Sci. Discuss., https://doi.org/10.5194/nhess-2018-75
Manuscript under review for journal Nat. Hazards Earth Syst. Sci.
Discussion started: 26 March 2018

Natural Hazards and Earth System Sciences
Discussions

GROWTH OF A SINKHOLE IN A SEISMIC ZONE OF THE NORTHERN APENNINES (ITALY)

Alessandro La Rosa[1,2], Carolina Pagli[2], Giancarlo Molli[2], Francesco Casu[3], Claudio De Luca[3], Amerino Pieroni[4]

[1] Dipartimento di Scienze della Terra, Università degli Studi di Firenze, Via G. La Pira, 4, 50121 Firenze, Italy

[2] Dipartimento di Scienze della Terra, Università di Pisa, Via S. Maria, 53, 56126 Pisa, Italy

[3] CNR, Consiglio Nazionale delle Ricerche, Istituto per il Rilevamento Elettromagnetico dell'Ambiente (IREA-CNR), Via Diocleziano, 328, 80124 Napoli, Italy

[4] Pro.Geo. s.r.l. Via Valmaira, 14, 55032, Castelnuovo di Garfagnana, Italy

Keywords: Sinkhole, InSAR, Seismicity

Abstract

Sinkhole collapse is a major hazard causing substantial social and economic losses. However, the surface deformations and sinkhole evolution are rarely recorded, as these sites are known mainly after a collapse, making the assessment of sinkholes-related hazard challenging. Furthermore, 40% of the sinkholes of Italy are in seismically hazardous zones; it remains unclear whether seismicity may trigger sinkhole collapse. Here we use a multidisciplinary dataset of InSAR, surface mapping and historical records of sinkhole activity to show that the Prà di Lama lake is a long-lived sinkhole that was formed over a century ago and grew through several events of unrest characterized by episodic subsidence and lake-level changes. Moreover, InSAR shows that continuous aseismic subsidence at rates of up to 7.1 mm yr^{-1} occurred during 2001-2008, between events of unrest. Earthquakes on the major faults near the sinkhole are not a trigger to sinkhole activity but small-magnitude earthquakes at 4-12 km depth occurred during sinkhole unrest in 1996 and 2016. We interpret our observations as evidence of seismic creep in an active fault zone at depth causing fracturing and ultimately leading to the formation and growth of the Prà di Lama sinkhole.

Nat. Hazards Earth Syst. Sci. Discuss., https://doi.org/10.5194/nhess-2018-75
Manuscript under review for journal Nat. Hazards Earth Syst. Sci.
Discussion started: 26 March 2018

Natural Hazards and Earth System Sciences
Discussions

1. Introduction

Sinkholes are quasi-circular depressions in the ground surface that form due to the breakdown of subterranean cavities (*Neuendorf et al., 2005*). Sinkhole subsidence and collapse cause substantial economic and human losses globally (*Frumkin and Raz, 2001*; *Wadas,* 2017; *Closson,* 2005). In Italy, a total of 750 sinkholes have been identified by *Caramanna et al*. (2008).

Typically, sinkholes form in karst landscapes where the exposed soluble rocks are dissolved by circulating ground water (dissolution sinkholes) but deep sinkholes also develop by erosion/dissolution of a deep layer of rock covered by non-soluble rocks (*Caramanna et al., 2008*). In particular, deep sinkholes have been observed along seismically active faults indicating a causal link between sinkhole formation and active tectonics (*Faccenna et al., 1993; Closson et al., 2005; Florea, 2005; Harrison et al., 2002; Wadas et al., 2017*). The processes responsible for the formation of these sinkholes have been attributed to fracturing and increased permeability in the fault damage zone promoting fluid circulation and weathering of soluble rocks at depth. Additionally, when carbonate bedrocks lie below thick non-carbonate formations, stress changes caused by faulting may cause decompression of confined aquifers favouring upward migration of deep acid fluids hence promoting erosion and collapses; a process known as Deep Piping (*Caramanna et al., 2008*). Sinkhole formation can also be triggered by faulting and two sinkholes formed near En Gedi, Dead Sea, following the M_w 5.2 earthquake on the Dead Sea Transform Fault in 2004 (*Salamon, 2004*).

The sinkhole of Prà di Lama, near the Pieve Fosciana town (Lucca, Italy), is a circular depression filled by a lake (*Caramanna et al., 2008*). Prà di Lama is located in the seismically active Apennine range of Northern Tuscany, at the intersection between two active faults (Fig. 1). Hot springs are also present at Pieve Fosciana suggesting that fluid migration along the faults planes

occurs. Sudden lake-level changes of up to several meters, ground subsidence, surface fracturing and seismicity have occurred repeatedly since at least 991 A.D. (*Nisio, 2008*). The most recent deformation events occurred in March 1996 and between May 2016 and October 2017. However, the processes that control the growth of the Prà di Lama sinkhole remain unclear. Furthermore, whether seismicity along the active faults around Pra di Lama may trigger sinkhole subsidence or collapse is debated.

In this paper we combine recent InSAR observations, seismicity, and surface mapping, as well as historical records of lake-level changes and ground subsidence at the Prà di Lama from 1828 to understand the mechanisms of sinkhole growth in an active fault system.

2. Geological Background

The area of the Prà di Lama sinkhole is located within the Garfagnana basin (Fig.1), an extensional graben in the western Northern Apennines, a NW-SE trending fold-and-thrust belt formed by the stack of different tectonic units caused by the convergence of the Corsica-European and Adria plates. the current tectonic regime of the Apennines is characterized by shortening in the eastern sector of the Apennine range and extension in the westernmost side of the range (*Elter et al., 1975; Patacca and Scandone, 1989; Bennett et al., 2012*). The contemporaneous eastward migration of shortening and upper plate extension are believed to be caused by the roll-back subduction during the counter-clockwise rotation of the Adria plate (*Doglioni, 1991; Meletti et al., 2000; Serpelloni et al., 2005; Faccenna et al., 2014; Le Breton et al., 2017 and references*). Extension started 4-5 Ma ago leading to the formation of several NW-SE-oriented grabens, bounded by NE-dipping and SW-dipping normal faults that are dissected by several NE-trending, right-lateral strike-slip faults (Fig. 1). The inner northern Apennines are a seismically active area, where several earthquakes with $M_W > 5$ occurred, including the largest instrumentally recorded earthquake, M_w 6.5, in 1920 (*Tertulliani and Maramai, 1998; Rovida et al., 2016; Bonini et al.,*

2016) and the most recent M_w 5.1 earthquake in 2013 (*Pezzo et al., 2014; Stramondo et al., 2014; Molli et al., 2016*).

The uppermost stratigraphy of the Prà di Lama sinkhole consists of an eight-meters-thick layer of alluvial and palustrine gravels and sandy deposits containing pity levels, covering ~60-m-thick sandy-to-silty fluvio-lacustrine deposits with low permeability (from Villafranchian to present age) (*Chetoni, 1995*). These recent deposits cover a turbiditic sequence named Macigno Fm. Below the Macigno Fm. a sequence of carbonate rocks pertaining to the Tuscan Nappe Unit is present.

The Prà di Lama sinkhole is located at the intersection between two seismically active faults: the Corfino normal fault (*Di Naccio et al., 2013*; *Itacha working group, 2003*; *ISIDe working group, 2016*) and the right-lateral strike-slip fault M.Perpoli-T.Scoltenna that recently generated the M_w 4.8 earthquake in January 2013 (Fig.1) (*Vannoli, 2013; Pinelli, 2013; Molli et al., 2017*). Hot water springs are also present at Prà di Lama and some of them have a water temperature of ~40 °C [32]. Prà di Lama was classified as a Deep Piping Sinkhole (DPS) as it is a circular depression that formed on thick impermeable sediments in a fracture zone, likely due to erosion of soluble rocks at depth (*Caramanna et al., 2008*). Hot springs are also a common feature of DPSs due to the presence of pressurized aquifers together with a system of fractures favouring fluid circulation.

3. Data

Century-scale historical records of sinkhole activity are available at Prà di Lama and allow us to determine the timescale of sinkhole evolution as well as to characterize the different events of unrest, in particular the two most recent events in 1996 and 2016. InSAR time-series analysis is also carried out to measure ground deformations in the Prà di Lama sinkhole in the time period between events of unrest. Finally, the local catalogue of seismicity (ISIDE catalogue, INGV) is used to inform us on the timing and types of brittle failures in the area of the sinkhole.

Nat. Hazards Earth Syst. Sci. Discuss., https://doi.org/10.5194/nhess-2018-75
Manuscript under review for journal Nat. Hazards Earth Syst. Sci.
Discussion started: 26 March 2018

99 **3.1 Historical Record**

100 The first historical record of the Prà di Lama sinkhole dates back to the 991 A.D., when the
101 area was described as a seasonal shallow pool fed by springs. Since then, the depression grew and
102 several events of unrest consisting of fracturing and fluctuations of the lake level were reported
103 (*Raffaelli, 1869; De Stefani, 1879, Giovannetti, 1975*) (Table 1). In Particular, eight events of unrest
104 were reported, giving an average of 1 event of unrest every 26 years. We conducted direct
105 observation of surface deformation around the lake for the two most recent events in 1996 and
106 2016.

107 In 1996, the lake level experienced a fall of up to 4 m (Fig. 2) and at the same time the
108 springs outside the lake suddenly increase the water outflow. Clay and mud were also ejected by
109 the springs outside the lake while fractures and slumps occurred within the lake due to the water
110 drop (Fig. 2). The unrest lasted approximately 2 months, from March to April 1996. During the final
111 stages, the water level in the lake rose rapidly recovering its initial level and contemporaneously
112 the springs water flow reduced.
113 In June 2016, an event of unrest consisting of ground subsidence on the western and southern
114 sides of the Prà di Lama lake started and lasted approximately 9 months, until February 2017.
115 During this period fractures formed and progressively grew, increasing their throw to up to 70 cm
116 and affecting a large area on the western side of the lake (Fig. 2). Subsidence around the lake
117 resulted in an increase of the lake surface in particular on the western side and formation of
118 tensile fractures (Fig. 2). Unlike the 1996 events of unrest, no lake level changes or increase of
119 water flow from the springs around the lake were observed.
120
121
122
123

3.2 InSAR

InSAR is ideally suited to monitor localized ground deformation such as caused by sinkholes as it can observe rapidly evolving deformation of the ground at high spatial resolution (*Baer et al., 2002; Castañeda et al., 2009; Abelson et al., 2017; Atzori et al., 2015*). Furthermore, the availability of relatively long datasets of SAR images in the Apennine allows us to study the behaviour of the Prà di Lama sinkhole using multi-temporal techniques. We processed a total of 200 interferograms using SAR images acquired by the ENVISAT satellite between 2003 to 2010 from two distinct tracks in Ascending or Descending viewing geometry (tracks 215 and 437). We used the Small BAseline Subset (SBAS) multi-interferogram method originally developed by *Berardino et al. (2002)* and recently implemented for parallel computing processing (P-SBAS) by *Casu et al. (2014*) to obtain incremental and cumulative time-series of InSAR Line-of-Sight (LOS) displacements as well as maps of average LOS velocity. In particular, the InSAR processing has been carried out via the ESA platform P-SBAS open-access on-line tool named G-POD (Grid Processing On Demand) that allows generating ground displacement time series from a set of SAR data (*De Luca et al*., *2015*).

The P-SBAS G-POD tool allows the user to set some key parameters to tune the InSAR processing. In this work, we set a maximum perpendicular baseline (spatial baseline) of 400 m and maximum temporal baseline of 1500 days. The geocoded pixel dimension was set to ~80 m by 80 m (corresponding to averaging together 20 pixels in range and 4 pixels in azimuth). We also set a coherence threshold to 0.8 (0 to 1 for low to high coherence) in order to select only highly coherent pixels in our interferograms. Excluding poorly coherent pixels reduces the noise in our final velocity maps and time-series (*De Luca et al., 2015*). We also inspected the series of interferograms and excluded individual interferograms with low coherence. We identified and discarded 29 noisy interferograms in track 215A and other 11 interferograms in track 437D. Finally, we applied an Atmospheric Phase Screen (APS) filtering to mitigate further atmospheric

disturbances (*Hassen, 2001*). Accordingly, we used a triangular temporal filter with a width of 400 days to minimize temporal variations shorter than about a year as we focus on steady deformations rather than seasonal changes. Shorter time interval of 300 days was also tested but provided more noisy time-series.

As a further post processing step (not yet available via the G-POD tool) we also calculated the vertical and east-west components of the velocity field in the area covered by both the ascending and descending tracks and assuming no north-south displacement. Given that the study area is imaged by the ENVISAT satellite from two symmetrical geometries with similar incidence angles (few degrees of difference), the vertical and east-west components of the velocity field can simply be obtained solving the following system of equations (*Manzo et al., 2006*):

$$\begin{cases} v_H = \dfrac{\cos\vartheta}{\sin(2\vartheta)}\,(v_{DESC} - v_{ASC}) = \dfrac{v_{DESC} - v_{ASC}}{2\sin\vartheta} \\ v_V = \dfrac{\sin\vartheta}{\sin(2\vartheta)}(v_{DESC} + v_{ASC}) = \dfrac{v_{DESC} + v_{ASC}}{2\cos\vartheta} \end{cases} \quad (158)$$

where v_H and v_V are the horizontal and vertical component of the velocity filed, v_{DESC} and v_{ASC} are the average LOS velocities in the Descending and Ascending tracks, respectively; ϑ is the incidence angle.

The InSAR P-SBAS analysis shows that significant surface deformation occurs at Pieve Fosciana between 2003 and 2010. The observed deformation pattern consists of range increase mainly on the western flank of the Prà di Lama lake. The range increase is observed in both ascending and descending velocity maps (Fig. 3a, b), with average LOS velocities of up to -7.1 mm yr^{-1} decaying to -1 mm yr^{-1} over a distance of 400 m away from the lake. Elsewhere around the lake coherence is not kept due to ground vegetation cover but few coherent pixels on eastern flank of the lake suggest that the deformation pattern may be circular, with a radius of ~600 m (Fig. 3e). The maps of vertical and East-West velocities show vertical rates of -4.6 mm yr^{-1} and horizontal

eastward velocities of 5.4 mm yr^{-1} (Fig. 3c, d) consistent with subsidence and contraction centred at the lake. Furthermore, figure 4 shows that the current deformation pattern follows the topography, suggesting that subsidence at Prà di Lama is a long-term feature. The time-series of cumulative LOS displacements show that subsidence occurred at an approximately constant rate between the 2003 and the 2008 but it slowed down in 2008 (Fig. 3e, f), indicating that subsidence at Prà di Lama occurs also between events of unrest. Furthermore, our time-series of vertical and east-west cumulative displacements also confirm that the fastest subsidence and contemporaneous eastward motion occurred until 2008 (Fig. 3 g, h). In order to better understand the mechanisms responsible for the sinkhole growth and the different types of episodic unrest we also analysed the seismicity.

3.3 Seismicity

We analysed the seismicity at the Prà di Lama lake using the catalogue ISIDe (Italian Seismological Instrumental and Parametric Data-Base) spanning the time period from 1986 to 2016. We calculated the cumulative seismic moment release using the relation between seismic moment and magnitudes given by *Kanamori* (1977). First, we analysed the seismic moment release and the magnitude content of the earthquakes in the area encompassing the sinkhole and the faults intersection (10 km radius, Fig. 1) to understand whether unrest at Prà di Lama is triggered by earthquakes along the active faults (Fig. 5). Fig. 4a shows that although several seismic swarms occurred in the area, no clear temporal correlation between the swarms and the events of unrest at Prà di Lama is observed, suggesting that the majority of seismic strain released on faults around the Prà di Lama lake does not affect the activity of the sinkhole. We removed from the plot in Fig. 4a the large magnitude earthquake, M_w 4.8, on the 25th of January 25, 2013 in order to better visualize the pattern of seismic moment release in time. In any case, no activity at Prà di Lama was reported in January 2013.

194 We also analysed the local seismicity around the Prà di lama lake, within a circular area of 3
195 km radius around the lake (Fig. 1), to better understand the deformation processes occurring at
196 the sinkhole (Fig. 6) and we found that swarms of small-magnitude earthquakes ($M_L \leq 2$) occurred
197 during both events of unrest at Prà di Lama in 1996 and 2016 (Fig. 6a, b, c), while a few
198 earthquakes with magnitudes > 2 occurred irrespective of the events of unrest. This indicates that
199 seismicity during sinkhole activity is characterized by seismic energy released preferentially
200 towards the small end of magnitudes spectrum. This pattern is specific of the sinkhole area as in
201 the broader region (Fig. 5b, c) the majority of earthquakes magnitudes are in the range between
202 $M_L > 2$ and $M_L < 3$ and few $M_L > 3$ also occurred. We also analysed the hypocentres of the
203 earthquakes around the Prà di lama lake (3 km radius) and find that these range between 4.5 and
204 11.5 km depth, indicating that deformation processes in the fault zone control the sinkhole
205 activity. On the other hand, no earthquakes were recorded at Prà di Lama during the period of
206 subsidence identified by InSAR between 2003 and 2010, indicating that subsidence between
207 events of unrest continuous largely aseismically.

208 4. **Discussion and conclusions**

209 A multi-disciplinary dataset of InSAR measurements, field observations and seismicity reveal
210 that diverse deformation events occur at the Prà di Lama sinkhole. Two main events of sinkhole
211 unrest occurred at Prà di Lama in 1996 and 2016 but the processes had different features. In 1996
212 the lake-level dropped together with increased water outflow from the springs, while in 2016
213 ground subsidence led to the expansion of the lake surface and fracturing. Furthermore, InSAR
214 analysis shows that continuous but aseismic subsidence of the sinkhole occurred between the two
215 events of unrest, during the period 2003-2010. Instead swarms of small-magnitude earthquakes
216 coeval to the unrest events of 1996 and 2016 were recorded at depth between 4.5 and 11.5 km,

indicating that a link between seismicity and sinkhole activity exists. We suggest that seismic creep in the fault zone underneath Prà di Lama occurs, causing the diverse deformation events. Seismic creep at depth could have induced pressure changes in the aquifer above the fault zone (1996 events) as well as causing subsidence by increased fracturing (2016 events). The seismicity pattern revealed by our analysis suggests that the Mt.Perpoli-T.Scoltenna strike-slip fault system underneath Prà di Lama is locally creeping, producing seismic sequences of low magnitude earthquakes. Similar seismicity patterns were observed in 2006 along the Superstition Hills fault (San Andreas fault system, California) where seismic creep is favoured by high water pressure (*Wei et al., 2009; Scholz, 1998; Harris, 2017*). We suggest that at the Prà di Lama fault zone an increase in pressure in the aquifer in 1996 caused fracturing at the bottom of the lake and upward migration of fluids rich in clays, in agreement with the observations of lake-level drop and mud-rich water ejected by the springs in 1996. Sudden fracturing and periods of compaction of cavities created by enhanced rock dissolution in the fluid circulation zone also explains both sudden subsidence and fracturing, as in 2016, and periods of continuous but aseismic subsidence as in 2003-2010. Similar processes have been envisaged for the formation of a sinkhole at the Napoleonville Salt Dome, where a seismicity study suggests that fracturing enhanced the rock permeability, promoting the rising of fluids and, as a consequence, erosion and creation of deep cavities prone to collapse (*Yarushina et al., 2017; Sibson, 1996; Micklethwaite et al., 2010, Nayak and Dreger, 2014*). Recently, a sequence of seismic events was identified at Mineral Beach (Dead Sea fault zone) and was interpreted as the result of cracks formation and faulting above subsurface cavities (*Abelson et al., 2017*).

Precursory subsidence of years to few months has been observed to precede sinkhole collapse in carbonate or evaporitic bedrocks (e.g. *Baer et al., 2002*; *Nof et al., 2013; Cathleen and Bloom, 2014; Atzori et al., 2015*; *Abelson et al., 2017*). However, the timing of these processes

241 strongly depends on the rheological properties of the rocks (*Shalev and Lyakhovsky, 2013*).
242 Furthermore, the presence of a thick lithoid sequence in Prà di Lama could mean that the sinkhole
243 will not collapse into the underlying cavities, also in agreement with the exceptionally long
244 timescale (~200 years) of growth of the Prà di Lama sinkhole (*Carammanna et al., 2008; Shalev*
245 *and Lykovsky, 2012; Abelson et al., 2017*). However, at present we are not able to establish if and
246 when a major collapse will occur in Prà di Lama.

247 We identified a wide range of surface deformation patterns associated with the Prà di Lama
248 sinkhole and we conclude that a source mechanism for the sinkhole formation and growth is
249 seismic creep in the active fault zone underneath the sinkhole. This mechanism could control the
250 evolution of other active DPSs in Italy as well as in other areas worldwide where sinkhole form in
251 active fault systems (e.g. Dead Sea area). InSAR monitoring has already shown to be a valid
252 method to detect precursory subsidence occurring before a sinkhole collapse and the recent SAR
253 missions, such as the European Sentinel-1, will very likely provide a powerful tool to identify such
254 deformations.

255

256

257

258

259

260

261

262

References

Abelson, M., Aksinenko, T., Kurzon, I., Pinsky, V., Baer, G., Nof, R., & Yechieli, Y.: Nanoseismicity forecast sinkhole collapse in the Dead Sea coast years in advance. https://doi.org/10.1130/G39579.1 (2017)

Atzori, S., Baer, G., Antonioli, A., & Salvi, S.: InSAR-based modelling and analysis of sinkholes along the Dead Sea coastline. Geophysical Research Letters, 42, 8383–8390. https://doi.org/10.1002/2015GL066053 (2015)

Bencini, A., Duchi, V., Martini, M.: Geochemistry of thermal springs of Tuscany (Italy). *Chemical Geology,* 19, 229-252. (1977)

Baer, G., Schattner, U., Wachs D., Sandwell, D., Wdowinski, S., Frydman, S.: The lowest place on Earth is subsiding – An InSAR (Interferomeric Synthetic Aperture Radar) Perspctive. Geological Society of America Bullettin, 114 (1), 12-23. https://doi.org/10.1130/00167606(2002)114<0012:TLPOEI>2.0.CO;2 (2002)

Bennet, R.A., Serpelloni, E., Hreinsdottir, S., Brandon, M.T., Buble, G., Basic T., Casale, G., Cavaliere, A., Anzidei, M., Marjonovic, Minelli, G., Molli, G., & Montanari, A.: Syn-convergent extension observed using the RETREAT GPS network, northern Apennines, Italy. *Journal of Geophysical Research*, *117*. https://doi.org/ 10.1029/2011JB008744 (2012)

Berardino, P., Fornaro, G., Lanari, R., & Sansosti, E.: A new algorithm for surface deformation monitoring based on Small Baseline Differential SAR interferograms. *IEEE International Geoscience and Remote Sensing Symposium*, *40*(11). https://doi.org/10.1109/TGRS.2002.803792 (2002)

Bonini, M., Corti, G., Donne, D. D., Sani, F., Piccardi, L., Vannucci, G., Genco, R., Martelli, L., Ripepe, M.: Seismic sources and stress transfer interaction among axial normal faults and external thrust fronts in the northern Apennines (Italy): a working hypothesis based on the 1916-1920 time-space cluster of earthquakes. Tectonophysics, 680, 67–89. https://doi.org/10.1016/j.tecto.2016.04.045 (2016)

Caramanna, G., Ciotoli, G., Nisio, S.: A review of natural sinkhole phenomena in Italian plain areas. *Natural Hazards*, *45*, 145–172. https://doi.org/10.1007/s11069-007-9165-7 (2008)

Castañeda, C., Gutiérrez, F., Manunta, M., Galve, J. P.: DInSAR measurements of ground deformation by sinkholes, mining subsidence, and landslides, Ebro River, Spain. *Earth Surf. Process. Landforms*, 34, 11, 1562–1574. https://doi.org/10.1002/esp.1848 (2009)

Casu, F., Elefante, S., Imperatore, P., Zinno, I., Manunta, M., De Luca, C., & Lanari, R: SBAS-DInSAR parallel processing for deformation time-series computation. *IEEE Journal of Selected Topics in Applied Earth Observations and Remote Sensing*, *7*(8), 3285–3296. https://doi.org/ 10.1109/JSTARS.2014.2322671 . (2014)

Cathleen, J., & Blom, R.: Bayou Corne, Louisiana, sinkhole: Precursory deformation measured by radar interferometry. Geology. 42 (2), 111-114. https://doi.org/10.1130/G34972.1 (2014)

Chetoni, R.: Terme di Prà di Lama (Pieve Fosciana, Lu), indagine geognostica sulle aree dissestate nel marzo 1996. Geological Report. (1996)

Closson, D.: Structural control of sinkholes and subsidence hazards along the Jordanian Dead Sea coast. Environvmental Geology, 47 (2), 290-301. https://doi.org/10.1007/s00254-004-1155-4 (2005)

Closson, D., Karaki, N.A., Klinger, Y., & Hussein, M. J.: Subsidence and Sinkhole Hazard Assessment in the Southern Dead Sea Area, Jordan. *Pure and Applied Geophysics*, *162*, 221–248. https://doi.org/10.1007/s00024-004-2598-y (2005)

De Luca, C., Cuccu, R., Elefante, S., Zinno, I., Manunta, M., Casola, V., Rivolta, G., Lanari, R., Casu, F.: An On-Demand Web Tool for the Unsupervised Retrieval of Earth's Surface Deformation from SAR Data: The P-SBAS Service within the ESA G-POD Environment. *Remote Sensing*, 7(11), 15630-15650. https://doi.org/10.3390/rs71115630 (2015)

De Stefani, C.: Le Acque Termali di Pieve Fosciana. *Memorie della Società Toscana di Scienze Naturali*, 4, 72-97 (1879)

Di Naccio, D., Boncio, P., Brozzetti, F., Pazzaglia, F. J., & Lavecchia, G.: Morphotectonic analysis of the Lunigiana and Garfagnana grabens (northern Apennines, Italy): Implications for active normal faulting. *Geomorphology*, *201*, 293–311. https://doi.org/10.1016/j.geomorph.2013.07.003 (2013)

Doglioni, C.: A proposal for the kinematic modelling of the W-dipping subduction – possible applications to the Tyrrhenian-Apennines system. Terra Nova, 3, 423-434. https://doi.org/10.1111/j.1365-3121.1991.tb00172.x (1991)

Elter, P., Giglia, G., Tongiorgi, M., Trevisan, L.: Tensional and compressional areas in the recent (Tortonian to Present) evolution of the Northern Apennines. *Bollettino di Geofisica Teorica ed Applicata*, 65 (8) (1975)

Faccenna, C. Florindo, F., Funiciello, R., Lombardi, S.: Tectonic setting and Sinkhole Features: case histories from Western Central Italy. *Quaternary Proceedings*, *3*, 47–56 (1993)

Faccenna, C. Becker, T.W., Miller, S.M., Serpelloni, E., & Willet, S.D.: Isostasy, dynamic topography, and the elevation of the Apennines of Italy. Earth and Planetary Science Letters, *407*, 163–174. https://doi.org/10.1016/j.epsl.2014.09.027 (1993)

Florea, L. J.: Using State-wide GIS data to identify the coincidence betwen sinkholes and geologic structure. *Journal of Cave and Karst Studies*, (August), 120–124. Retrieved from http://digitalcommons.wku.edu/geog_fac_pub/14 (2005)

Frumkin, A., & Raz, E.: Collapse and subsidence associated with salt karstification along the Dead Sea. *Carbonates and Evaporites*, *16*(2), 117–130. https://doi.org/https://doi.org/10.1007/bf03175830 (2001)

Giovannetti, F.: Pieve Fosciana Ieri e Oggi. (1975)

Hanssen, R. F.: Radar Interferometry: Data Interpretation and Error Analysis. Kluwer Academic Publisher. https://doi.org/10.1007/0-306-47633-9 (2001)

Harris, R.A.: Large earthquakes and creeping faults. *Reviews of Geophysics*, 55, 169-198. https://doi.org/10.1002/2016RG000539 (2017)

Harrison, R. W., Newell, W. L., & Necdet, M.: Karstification Along an Active Fault Zone in Cyprus. Atlanta, Georgia. *U.S. Geological Survey Water-Resources Investigations Report* 02-4174 (2002)

ISIDe working group version 1.0 (2016)

Johnson, A. G., Kovach, R. L., & Nur, A.: Pore pressure changes during creep events on the San Andreas Fault. *Journal of Geophysical Research,* 78 (5). https://doi.org/10.1029/JB078i005p00851 (1973)

Kanamori, H.: The Energy Release in Great Earthquakes. *Journal of Geophysical Research*, *82*(20). https://doi.org/10.1029/JB082i020p02981 (1977)

Le Breton, E., Handy, M., Molli, G., & Ustaszewski K.: Post-20 Ma Motion of the Adriatic Plate: New Constraints from Surrounding Orogens and Implications for Crust-Mantle Decoupling. Tectonics, 36. https://doi. org/10.1002/2016TC004443 (2000)

Manzo, M., Ricciardi, G.P., Casu F., Ventura, G., Zeni, G., Borgström S., Berardino, P., Del Gaudio, C., Lanari, R.: Surface deformation analysis in th Ischia Island (Italy) based on spaceborne radar interferometry. Journal of Volcanology and Geothermal Research 151, 399-416. https://doi.org/10.1016/j.jvolgeores.2005.09.010 (2006)

Meletti, C., Patacca, E., & Scandone P.: Construction of a Seismotectonic Model: The Case of Italy. *Pure and applied Geophysics*, 157, 11-35. https://doi.org/10.1007/PL00001089 (2000)

Micklethwaite, S., Sheldon, H. A., & Baker, T.: Active fault and shear processes and their implications for mineral deposit formation and discovery. *Journal of Structural Geology*, *32*(2), 151–165. https://doi.org/10.1016/j.jsg.2009.10.009 (2010)

Molli, G., Torelli, L., & Storti, F.: The 2013 Lunigiana (Central Italy) earthquake: Seismic source analysis from DInSar and seismological data, and geodynamic implications for the northern Apennines. A discussion. Tectonophysics, 668–669, 108–112. http://dx.doi.org/10.1016/j.tecto.2015.07.041 (2016)

Molli, G., Pinelli, G., Bigot, A., Bennett R., Malavieille J., Serpelloni E.: Active Faults in the inner northern Apennines: a multidisciplinary reappraisal. From 1997 to 2016: Three Destructive Earthquakes along the Central Apennnine Fault system, Italy. July 19th-22nd 2017 Camerino, Volume Abstract (2017)

Nayak, A., & Dreger, D. S.: Moment Tensor Inversion of Seismic Events Associated with the Sinkhole at Napoleonville Salt Dome, Louisiana. *Bullettin of the Seismological Society of America*, 104(4), 1763–1776. https://doi.org/10.1785/0120130260 (2014)

Neuendorf, K., Mehl, J., Jackson, J.: Glossary of geology, 5th edn. *American Geological Institute*, 779 pp. (2005)

Nisio, S.: The sinkholes in Tuscany Region. *Memorie Descrittive Carta Geologica d'Italia LXXXV* (2008)

Nof, R. N., Baer, G., Ziv, A., Raz, E., Atzori, S., & Salvi, S.: Sinkhole precursors along the Dead Sea, Israel, revealed by SAR interferometry. *Geology,* 41, (9), 1019-1022. https://doi.org/10.1130/G34505.1 (2013)

Patacca, E., & Scandone, P.: Post-Tortonian mountain building in the Apennines, the role of the passive sinking of a relic lithospheric slab. The Lithosphere in Italy, 157–176 (1989).

373 Pezzo, G., Boncori, J.P.M., Atzori, S., Piccinini, D., Antonioli, A., Salvi, S.: The 2013 Lunigiana (Central Italy)
374 earthquake: Seismic source analysis from DInSAR and seismological data, and geodynamical
375 implications for the northern Apennines. Tectonophysics 636, 315–324.
376 http://dx.doi.org/10.1016/j.tecto.2014.09.005. (2014)
377
378 Pinelli, G.: Tettonica recente e attiva nell'Appennino interno a Nord dell'Arno: una revisione delle strutture
379 e delle problematiche. Diploma Thesis (89 pp) (2013)

380 Raffaelli, R.: Sulle acque termali di Pieve Fosciana (1869)

381 Rovida A., Locati M., Camassi R., Lolli B., Gasperini P.: CPTI15, the 2015 version of the Parametric Catalogue
382 of Italian Earthquakes. *Istituto Nazionale di Geofisica e Vulcanologia*. http://doi.org/10.6092/INGV.IT-
383 CPTI15 (2016)

384 Salamon, A.: Seismically induced ground effects of the February 11, 2004, M L = 5.2, North-eastern Dead
385 Sea earthquake. *Geological Survey of Israel Report* (2004)

386 Serpelloni, E., Anzidei, M., Baldi, P., Casula, G., & Galvani, A.: Crustal velocity and strain -rate fields in Italy
387 and surrounding regions: New results from the analysis of permanent and non-permanent GPS
388 networks. *Geophysical Journal International*, 161(3), 861–880.
389 https://doi.org/10.1016/j.epsl.2014.03.005 (2005)

390 Shalev, E., & Lyakhovsky, V.: Viscoelastic damage modeling of sinkhole formation. *Journal of Structural*
391 *Geology*, *42*, 163–170. https://doi.org/10.1016/j.jsg.2012.05.010 (2012)

392 Scholz, C. H.: Earthquakes and friction laws. *Nature*, 391, 37–42. https://doi.org/10.1038/34097 (1998)

393 Sibson, R. H.: Roughness at the Base of the Seismogenic Zone: Contributing Factors. *Journal of Geophysical*
394 *Research,* 87 (B7), 5791-5799. https://doi.org/10.1029/JB089iB07p05791 (1984)

395 Sibson, R. H.: Structural permeability of fluid-driven fault-fracture meshes. Journal of Structural Geology, 18
396 (8),1031-1042. https://doi.org/10.1016/0191-8141(96)00032-6 (1996)

397 Stramondo, S., Vannoli, P., Cannelli, V., Polcari, M., Melini, D., Samsonov, S., Moro, M., Bignami, C., & Saroli,
398 M.: X- and C-band SAR surface displacement for the 2013 Lunigiana earthquake (Northern Italy): a
399 breached relay ramp? IEEE J. Sel. Top. Appl. Earth Obs. Remote Sens.
400 http://dx.doi.org/10.1109/JSTARS.2014.2313640 (2014)

401 Tertulliani, A., & Maramai, A.: Macroseismic evidence and site effects for the Lunigiana (Italy) 1995
402 Earthquake. *Journal of Seismology*, 2 (3), 209–222. https://doi.org/10.1023/A:1009734620985 (1998)

403 Vannoli, P.: Il terremoto in Garfagnana del 25 gennaio 2013 visto dal geologo. Retrieved from
404 https://ingvterremoti.wordpress.com/2013/02/06/il-terremoto-del-25-gennaio-2013-visto-dal-
405 geologo/#more-3132 (2013)

406 Wadas, S. H., Tanner, D. C., Polom, U., & Krawczyk, C. M.: Structural analysis of S-wave seismics around an
407 urban sinkhole; evidence of enhanced suberosion in a strike-slip fault zone. *Natural Hazards and Earth*
408 *System Sciences.* https://doi.org/10.5194/nhess-2017-315 (2017)

409 Wei, M., Sandwell, D., & Fialko, Y.: A silent Mw 4.7 slip event of October 2006 on the Superstition Hills fault,
410 southern California. *Journal of Geophysical Research*, 114, B07402,
411 https://doi.org/10.1029/2008JB006135 (2009)

412 Yarushina, V. M., Podladchikov, Y.Y., Minakov, A., & Räss, L.: On the Mechanisms of Stress-Triggered
413 Seismic Events during Fluid Injection. *Sixth Biot Conference on Poromechanics, American Society of*
414 *Civil Engineers.* https://doi.org/10.1061/9780784480779.098 (2017)

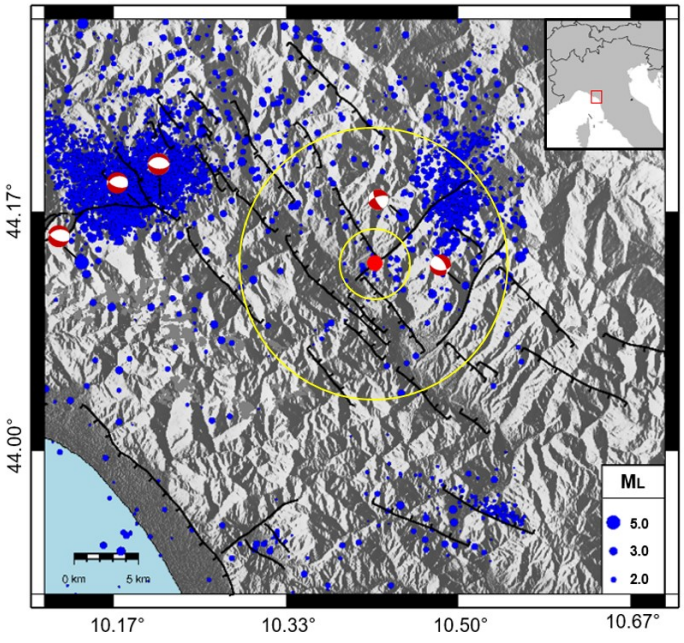

415
416 ***Figure 1 - Study area***. The Pieve Fosciana area is marked by the red dot. Black tick lines are faults. Blue dots are the earthquakes
417 between 1986 and 2017. Focal mechanisms are from the Regional Centroid Moment Tensor (RCMT) catalogue. The yellow circles
418 represent the areas with radii of 3km and 10 km used for the seismicity analysis. The red box in the *in*set marks the location of the
419 area shown in the main figure.

Nat. Hazards Earth Syst. Sci. Discuss., https://doi.org/10.5194/nhess-2018-75
Manuscript under review for journal Nat. Hazards Earth Syst. Sci.
Discussion started: 26 March 2018

Natural Hazards and Earth System Sciences
Discussions

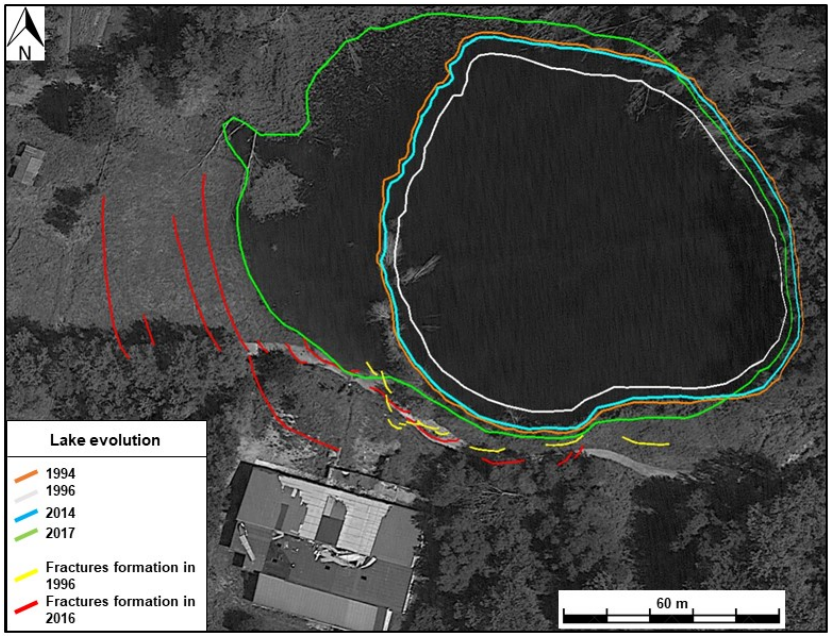

Figure 2 *– **Evolution of the Prà di Lama lake between 1994 and 2017**.* Lake shores variation have been retrieved from the analysis of Landsat image

Nat. Hazards Earth Syst. Sci. Discuss., https://doi.org/10.5194/nhess-2018-75
Manuscript under review for journal Nat. Hazards Earth Syst. Sci.
Discussion started: 26 March 2018

Natural Hazards and Earth System Sciences
Discussions

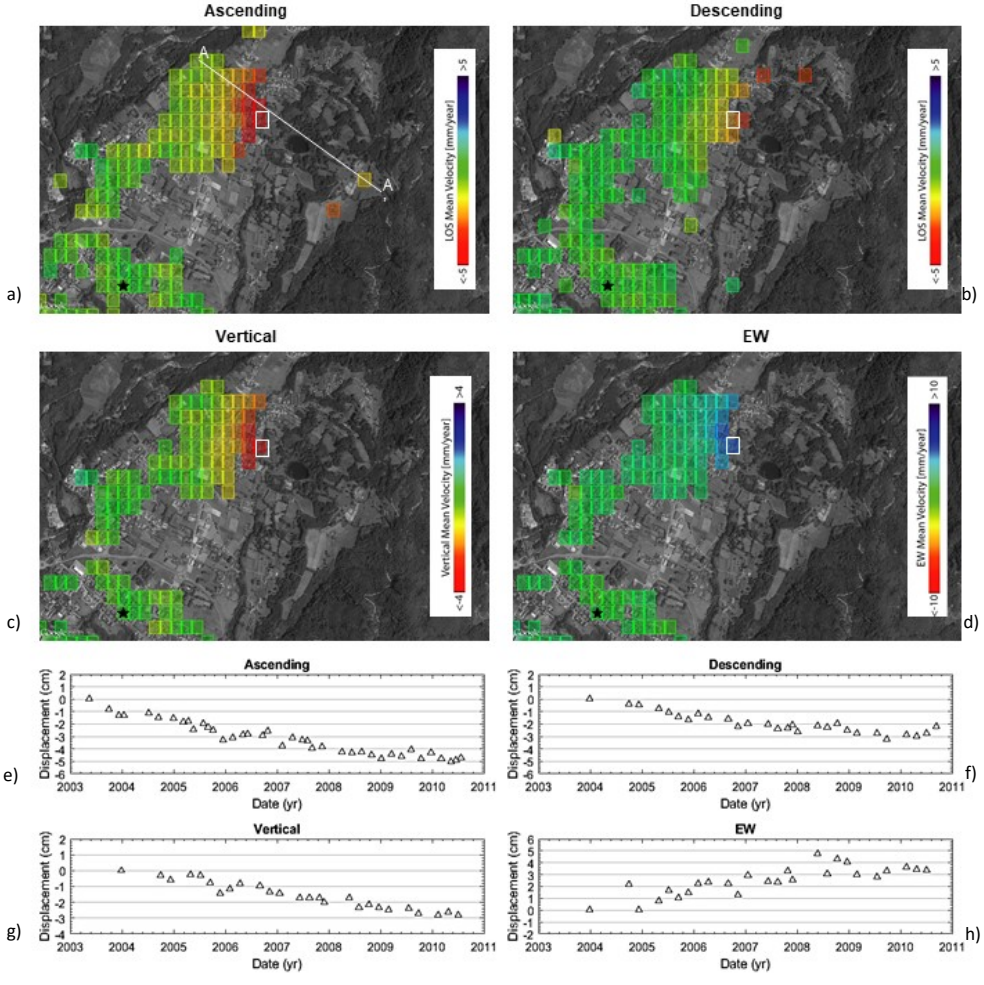

Figure 3 – a, b) Maps of average surface velocity and its vertical **(c)** and East-West **(d)** components obtained from ENVISAT SAR images acquired between 2003 and 2010. Negative values indicate range increase. The white line in panel a) marks the cross-section shown in figure 4. The black star is the point used as reference for the InSAR-SBAS processing. **e, f, g, h)** Time-series of incremental deformation extracted from the pixel bounded with the white rectangle.

Nat. Hazards Earth Syst. Sci. Discuss., https://doi.org/10.5194/nhess-2018-75
Manuscript under review for journal Nat. Hazards Earth Syst. Sci.
Discussion started: 26 March 2018

Natural Hazards and Earth System Sciences
Discussions

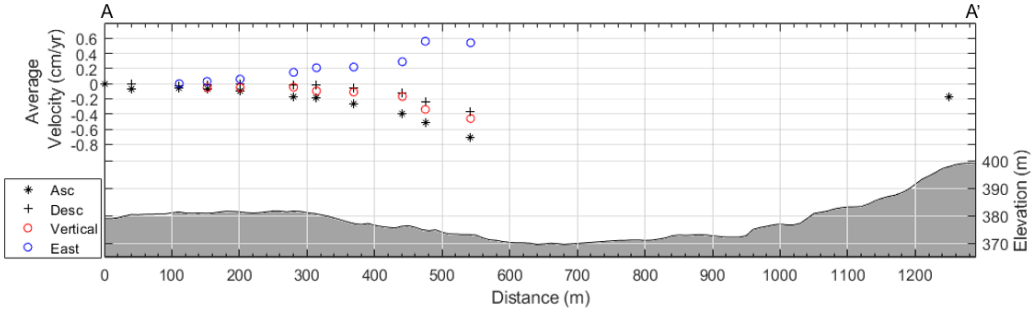

Figure 4 - ***Cross-section of topography and InSAR velocities along the A-A' profile as shown in figure 3a.***

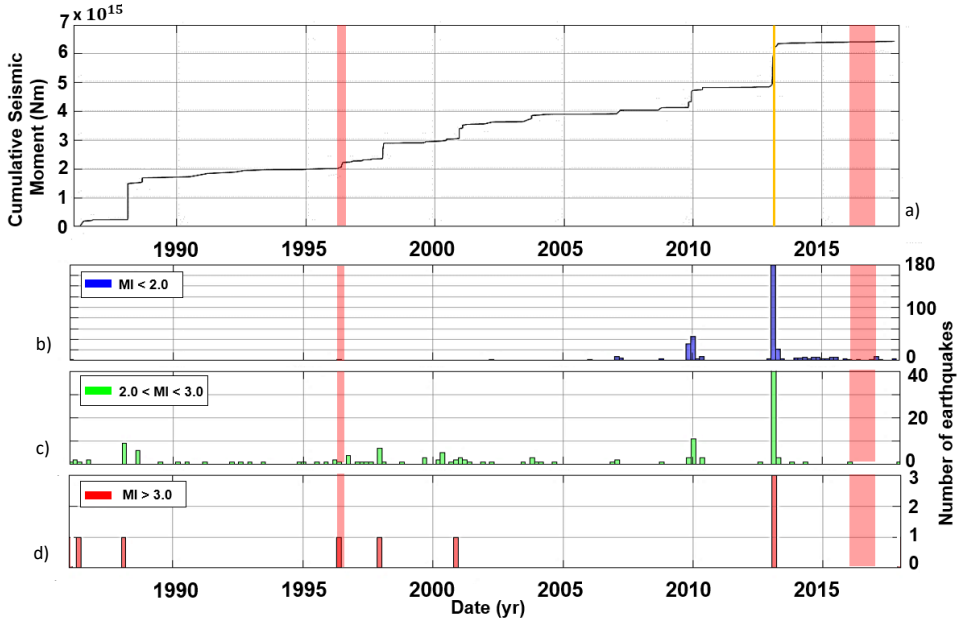

Figure 5 – Seismicity within a 10 km radius area around the Prà di Lama lake. cumulative seismic moment released in the area **(a)** and histograms of the number of earthquakes per month. Three different classes of magnitude have been created: Ml < 2.0 **(b)**, 2.0 < Ml < 3.0 **(c)** and Ml > 3.0 **(d)**. The dataset covers the period between 1986 and 2017.

Nat. Hazards Earth Syst. Sci. Discuss., https://doi.org/10.5194/nhess-2018-75
Manuscript under review for journal Nat. Hazards Earth Syst. Sci.
Discussion started: 26 March 2018

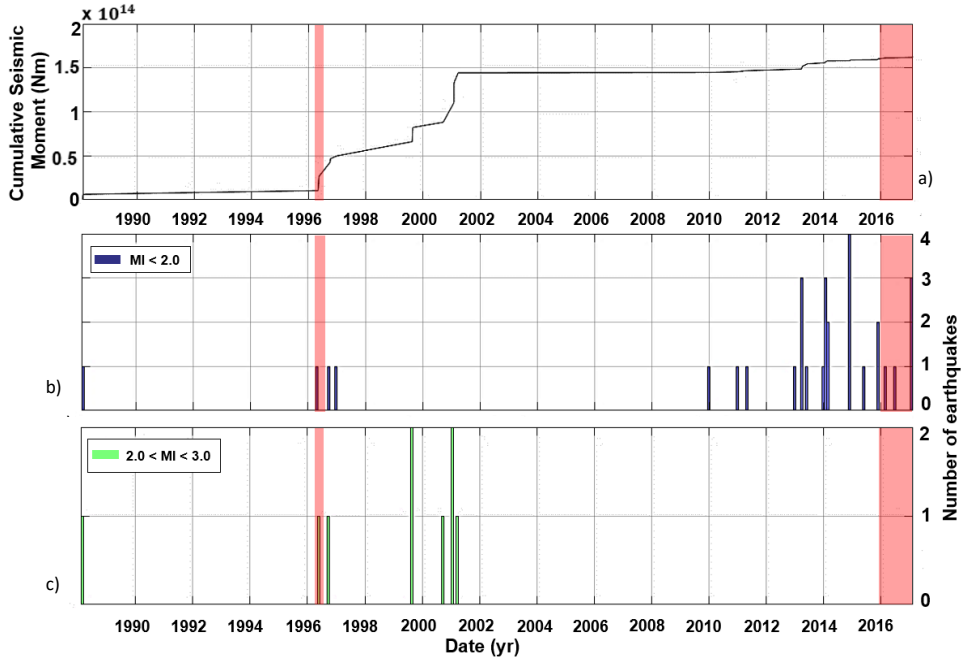

439

440 ***Figure 6 - Seismicity features of an area 3 km in radius around the Prà di Lama lake***. Plot of the cumulative seismic moment
441 released in the area **(a)** and histograms showing the number of earthquakes occurred each month. Two different classes of
442 Magnitude have been created: Ml < 2.0 **(b)**, 2.0 < Ml < 3.0 **(c)**. No events of Ml > 3.0 occurred in the area between 1986 and 2017.

Year	Brief description of the event
991	Seasonal pool fed by springs
1828	Bursts of the springs water flow. Uprising of muddy waters and clays (*Raffaelli, 1869; De Stefani, 1879*)
1843	Bursts of the springs water flow. Uprising of muddy waters and clays (*Raffaelli, 1869; De Stefani, 1879*)
1876	Subsidence and fracturing (*De Stefani, 1879*)
1877	Subsidence and fracturing (*De Stefani, 1879*)
1962	Bursts of the spring water flow. Uprising of muddy waters and clays (*Giovannetti, 1975*)
1969	Abrupt falling of the water level and fracturing along the shores. The lake almost disappeared (*Giovannetti, 1975*)
1985	Arising of muddy waters in a well
1996	Abrupt fall of the water level and fracturing along the shores
2016-2017	Subsidence and fracturing

443 ***Table 1 – Description of the activity at Prà di Lama lake***